

Tungsten Carbide-Cobalt Particles Activate Nrf2 and Its Downstream Target Genes in JB6 Cells Possibly by ROS Generation

*Xing-Dong Zhang,^{§,1,2} Jinshun Zhao,^{§,2} Linda Bowman,² Xian-
glin Shi,¹ Vincent Castranova,² & Min Ding^{2,*}*

¹Graduate Center for Toxicology, University of Kentucky, Lexington, KY 40515; ²Pathology and Physiology Research Branch, Health Effects Laboratory Division, National Institute for Occupational Safety and Health, 1095 Willowdale Road, Morgantown, WV 26505

[§]Equal contributors.

*Corresponding author. E-mail: mid5@cdc.gov

Hard metal consisting of a mixture of tungsten carbide (WC) and metallic cobalt (Co) was evaluated as a possible carcinogen in humans by IARC in 2003. Studies have suggested that nuclear factor erythroid 2-related factor 2 (Nrf2) constitutes one of the chemical-sensing and transcription systems that play an essential role(s) in chemical toxicity, carcinogenesis, and pathological processes. To elucidate the mechanisms of health hazards of WC-Co, effects of nano-WC-Co particles on Nrf2 signaling pathway were investigated in the present study in a JB6 cell line. After a 5 h treatment with nano-WC-Co particles, Nrf2 was released from Keap1 in the cytoplasm and translocated into the nucleus. Enzymatic activities of Nrf2 target genes, including glutathione S-transferase (GST) and NAD(P)H:quinone oxidoreductase 1 (NQO1), increased at 24 and 48 h after the treatment. Studies using reactive oxygen species (ROS) sensitive dyes indicated that ROS were produced in nano-WC-Co particle-treated cells. Pretreatment of the cells with catalase, but not sodium formate, resulted in a significant inhibitory effect on nano-WC-Co particle-induced Nrf2 target gene activation. These findings suggest that activation of Nrf2 and its downstream genes may be initiated by ROS generation, and ROS may act as a major contributor in nano-WC-Co particle-induced adverse health effects.

KEY WORDS: tungsten carbide-cobalt (WC-Co), cancer; nanoparticles, reactive oxygen species (ROS), nuclear factor erythroid 2-related factor 2 (Nrf2)

Introduction

Tungsten (or wolfram) carbide (WC) and metallic cobalt (Co) are important industrial materials due to their extreme hardness and high wear-resistance properties. Co is considered the offending agent in the WC-Co mixture alloy.¹ Occupational exposure of workers to the WC-Co particle mixture has been shown to be carcinogenic, and Co itself can also induce occupational asthma.²⁻⁴ Nanosized WC-Co (nano-WC-Co) was recently introduced in industry⁵ for the improved hardness and toughness compared to standard WC-Co materials mentioned above. However, the health effects of exposure to nano-WC-Co particles are unknown. Furthermore, the molecular events mediating cellular responses to nano-WC-Co particles also remain to be elucidated.

Nrf2 is a redox-sensitive basic leucine zipper transcription factor. This factor is involved in the transcriptional regulation of many detoxifying and antioxidant genes in different tissues, such as liver and kidney.^{6,7} Nrf2 has a special role in various physiological stress conditions, such as oxidative stress caused by ROS. Cells may be predisposed to chemical carcinogenesis if Nrf2 activity levels are too low. However, elevated Nrf2 activity may also play a role in the evolution of cancer.^{8,9}

Human beings are exposed to a large number of xenobiotics everyday from the occupational environment in a variety of industries as well as from nonoccupational environments. As a result, complex systems have evolved using enzymes for detoxification and protection. Generally, there are three xenobiotic metabolizing systems for the process of detoxification: Phase I involves oxidation of xenobiotics, phase II conjugation of the phase I products, and phase III is the ATP-dependent glutathione S-conjugate export pump.¹⁰ Nrf2 plays an essential role for the transcriptional induction of its downstream target genes, such as glutathione S-transferase (GST) and NAD(P)H:quinone oxidoreductase 1 (NQO1), protecting against toxicity or oxidative stress.^{7,11-13} When mammalian cells are exposed to stimulants that induce oxidative stress, such as ROS or various chemicals, a set of antioxidative stress proteins and phase II xenobiotic detoxifying enzymes of GST and NQO1 are induced.^{7,14} The signaling pathways controlling the activation of Nrf2 and subsequent ARE-mediated transcription have been elucidated by several studies.^{15,16} Keap1, a cytoplasmic actin-bind-

ing protein, is an inhibitor of Nrf2 that retains it as a Keap1-Nrf2 complex in the cytoplasm.¹⁷ When some insults stimulate the interaction of the complex, Nrf2 will be released from the complex. The Nrf2 will then translocate into the nucleus, bind to ARE, and regulate transcription of its downstream target genes for phase II enzymes. To elucidate the mechanisms of health hazards of WC-Co, effects of nano-WC-Co particles on Nrf2 signaling pathway were investigated in the present study in a JB6 cell line.

Materials and Methods

Materials

Nano-WC-Co particles (99.9% pure, molecularly mixed at the ratio of 85:15, agglomerated powder) were purchased from Inframat[®] Advanced Materials TM LLC (Farmington, CT). Eagle's minimum essential medium (EMEM) and phosphate buffered saline (PBS) were obtained from Lonza (Walkersville, MD). Fetal bovine serum (FBS), trypsin, penicillin/streptomycin, and L-glutamine were purchased from Life Technologies, Inc. (Gaithersburg, MD). Alexa Fluor 488 donkey antigoat IgG, 4',6-diamidino-2-phenylindole (DAPI), 2',7'-dichlorodihydrofluorescein diacetate (H2DCFDA), and dihydroethidium (DHE) were purchased from Molecular Probes (Eugene, OR). Luciferase assay substrate was purchased from Promega (Madison, WI). Catalase was purchased from Roche Molecular Biochemicals (Indianapolis, IN). Protease inhibitor cocktail, deferoxamine (DFO), N-acetyl-cysteine (NAC), poly-2-vinylpyridine-N-oxide (PVPNO), superoxide dismutase (SOD), and sodium formate were purchased from Sigma Chemical Co. (St. Louis, MO). Protein A/G plus-agarose beads and all other antibodies were obtained from Santa Cruz Biotechnology Co. (Santa Cruz, CA).

Preparation of Nano-WC-Co Particles

Stock solutions of nano-WC-Co particles were prepared by sonification on ice using a Branson Sonifier 450 (Branson Ultrasonics Corp., Danbury, CT) in sterile PBS (10 mg/ml) for 30 s, then kept on ice for 15 s and sonicated again for a total of 3 min at a power of 400 W. Before use, these particles were diluted to a designed concentration in fresh culture medium. All samples were prepared under sterile conditions. The average surface area and size of nano-WC-Co

particles were 2.73 m²/g and 95.53 nm, respectively, which were measured using a Gemini 2360 surface area analyzer (Micromeritics, Norcross, GA) or a scanning electron microscopy (SEM), respectively.

Cell Culture

Mouse epidermal JB6 cells were maintained in 5% FBS EMEM containing 2 mM L-glutamine and 1% penicillin-streptomycin (10,000 U/ml penicillin and 10 mg/ml streptomycin) at standard culture conditions (37°C, 80% humidified air, and 5% CO₂). For all treatments, cells were grown to 80% confluence.

Western Blot

Briefly, JB6 cells were plated onto a 6-well plate. Cells were grown 24 h and then starved in 0.1% FBS EMEM overnight. Cells were treated with/without various concentrations of nano-WC-Co particles for 5 h. After treatment, cells were extracted with 1 X SDS sample buffer supplemented with protease inhibitor cocktail. Protein concentration was determined using the bicinchoninic acid (BCA) protein assay method. Equal amounts of proteins were separated by 4–12% Tris-glycine gels. Immunoblot for expression of Nrf2 was detected. Experiments were performed three or more times, and equal loading of protein was ensured by measuring beta-actin.

Nuclear Extracts

Nuclear extracts from JB6 cells were prepared as described previously.¹⁸ Briefly, harvested cells were suspended in hypotonic buffer A [10 mM HEPES (pH 7.6), 10 mM KCl, 0.1 mM EDTA, 1 mM dithiothreitol, and 0.5 mM phenylmethylsulfonyl fluoride] for 10 min on ice and then vortexed for 10 s. Nuclei were pelleted by centrifugation at 12,000 × g for 20 s and then resuspended in buffer B [20 mM HEPES (pH 7.6), 25% glycerol, 0.4 M NaCl, 1 mM EDTA, 1 mM dithiothreitol, and 0.5 mM phenylmethylsulfonyl fluoride] for 30 min on ice. The supernatants containing nuclear proteins were collected after centrifugation at 12,000 × g for 2 min.

Immunocytochemistry Staining

JB6 cells were grown on sterilized cover slips until 60–80% confluent. Then, cells were treated with/with-

out nano-WC-Co particles for 5 h. Cells were fixed with 4% para-formaldehyde in PBS, permeabilized with 0.5% Triton X-100/PBS for 30 min, and blocked with 3% bovine serum albumin in PBS for 1 h at 37°C. The cells were then incubated with Nrf2 antibody at 4°C overnight. After washing with PBS, Alexa Fluor 488 secondary antibody supplemented with DAPI (2 µg/ml) was added. Cells were incubated at room temperature for 90 min. Fluorescence images were acquired with an immunofluorescence microscope.

Immunoprecipitation (IP) Western Blot

After treatment, cells were lysed in radioimmune precipitation assay buffer (50 mM Tris-HCl, pH 7.4, with 1% nonidet P-40, 0.25% sodium deoxycholate, 1 mM EDTA, protease and phosphatase inhibitors). Lysates were centrifuged at 12,000 × g for 15 min. Protein concentrations of the supernatants were determined. Equal amounts of proteins were pre-cleared with protein A/G plus-agarose beads for 1 h at 4°C, followed by incubation with protein A/G plus-agarose beads and Nrf2 antibody at 4°C overnight with shaking. Beads were pelleted, washed three times in PBS with 0.05% Tween 20 (PBST) buffer, and finally boiled in 1X SDS sample buffer. Proteins were separated by 4–12% Tris-glycine gels. Then, immunoblotting (IB) using antibody against Keap1 was conducted.

Measurement of GST A1 ARE-Luciferase Activity

JB6 cells, stably transfected with the GST A1 ARE-luciferase plasmid, were seeded onto a 24-well plate. Cells (5 × 10⁴ in 1 ml of culture medium) were grown 24 h and then starved in 0.1% FBS EMEM overnight. Cells were treated with/without various concentrations of nano-WC-Co particles for 24 h. To test the involvement of ROS in nano-WC-Co particle-induced Nrf2 activation, effects of antioxidants on GST A1 ARE-luciferase activity were investigated. JB6 cells were pretreated with different antioxidants for 1 h, and then cells were exposed to nano-WC-Co particles for 20 h. Thereafter, cells were lysed with 100 µl of luciferase lysis buffer (Promega). The luciferase activity of GST A1 ARE was measured by addition of luciferase assay substrate using a luminometer (Monolight® 3010, Analytical Luminescence Laboratory, San Diego, CA).

Enzyme Activity Assay

The activities of the detoxifying phase II enzymes (GST and NQO1) were measured spectrophotometrically based on previous established methods.¹⁹ For detection of GST activity, JB6 cells were grown in a 96-well plate and treated with/without nano-WC-Co particles for 48 h. Then, cells were lysed with 200 μ l of lysis buffer [0.25 M sucrose, 10 mM Tris-HCl (pH 7.5), 1 mM EDTA, 0.5 mM dithiothreitol, 0.5 mM phenylmethylsulfonyl fluoride, and 1% Triton X-100] for 30 min. Assays were conducted in a thermostated compartment at 25°C. Cytosolic protein (45 μ g) was added to 800 μ l of reaction mixture containing 100 mM KH_2PO_4 (pH 6.5) and 1 mM glutathione. The reaction was initiated by adding 1 mM chloro-2-4-dinitrobenzene (CDNB), and the formation of thioether after 5 min was measured at 340 nm. Total enzymatic activity of GST was expressed as ratios of treated over vehicle control. For detection of NQO1 activity, the cells were grown in a 96-well plate, treated with various concentrations of nano-WC-Co particles for 48 h and lysed with 0.8% digiton. The reaction solution [25 mM Tris-HCl (pH 7.4), 0.06% bovine serum albumin, 5 μ M flavin adenine (FAD), 1 mM glucose 6-phosphate, 30 μ M beta-nicotinamide adenine dinucleotide phosphate (NADP), 300 units of glucose-6-phosphate dehydrogenase, 725 μ M 3-(4,5-dimethylthiazol-2-yl)-2,5-diphenyltetrazolium bromide, and 50 μ M menadione] was added into each well and reduced 3-(4,5-dimethylthiazol-2-yl)-2,5-diphenyltetrazolium bromide was measured at 610 nm. NQO1 induction by nano-WC-Co particles was expressed as ratios of treated over vehicle control.

General ROS and $\text{O}_2^{\cdot -}$ Detection in Intact Cells

H2DCFDA and DHE are specific dyes used for staining general ROS and $\text{O}_2^{\cdot -}$, respectively, produced by intact cells. JB6 cells were seeded into a 24-well plate. Cells were grown 24 h and then starved in 0.1% FBS EMEM overnight. Thereafter, cells were treated with/without various concentrations of nano-WC-Co particles in the presence of H2DCFDA (5 μ M) and DHE (2 μ M) for 1 h. The cells were washed three times with PBS, followed by addition of fresh 0.1% FBS EMEM. The images were captured with an immunofluorescence microscope.

Statistical Analysis

Data are presented as means \pm standard errors (S.E.) as noted in the figure legends. Significant differences were determined using the Student's t-test. Significance was set at $p \leq 0.05$.

Results

Nuclear Translocation of Nrf2 after Nano-WC-Co Particle Exposure

To determine the changes of localization and translocation of Nrf2 following exposure to nano-WC-Co particles, western blot and immunocytochemistry staining were performed. As shown in Fig. 1A, western blot showed that Nrf2 was significantly enhanced in the nuclei of cells treated with nano-WC-Co particles. The nucleus translocation of Nrf2 reached a peak at 25–50 $\mu\text{g}/\text{cm}^2$ of nano-WC-Co particles. Nrf2 contents in the whole cells were not significantly affected by exposure to different concentrations of nano-WC-Co particles. Immunocytochemistry staining (Fig 1B) showed that the Nrf2 was translocated in the nuclei after 5 h exposure to 25 and 100 $\mu\text{g}/\text{cm}^2$ of nano-WC-Co particles.

Dissociation of Keap1-Nrf2 Complexes

To study the dissociation of Keap1-Nrf2 complexes, IP using antibody against Nrf2 to obtain Keap1-Nrf2 complexes followed by Immunoblotting (IB) using antibody against Keap1 was conducted. Cells without treatment (negative control) showed the lowest amounts of dissociation of Keap1-Nrf2 complexes compared to tBHQ (positive control) and nano-WC-Co particle treatments. Nano-WC-Co particles induced a dose-dependent increase of the dissociation of Keap1-Nrf2 complexes (Fig 2).

Activities of Phase II Enzymes

To evaluate the expression of detoxifying phase II enzymes following treatment with nano-WC-Co particles, enzymatic activities of GST and NQO1 were measured. As shown in Fig. 3A, nano-WC-Co particles induced an increase of GST A1 ARE luciferase activity in a dose-dependent manner. Measurements with spectrophotometry showed levels of the enzymatic activities of both total GST and NQO1 were

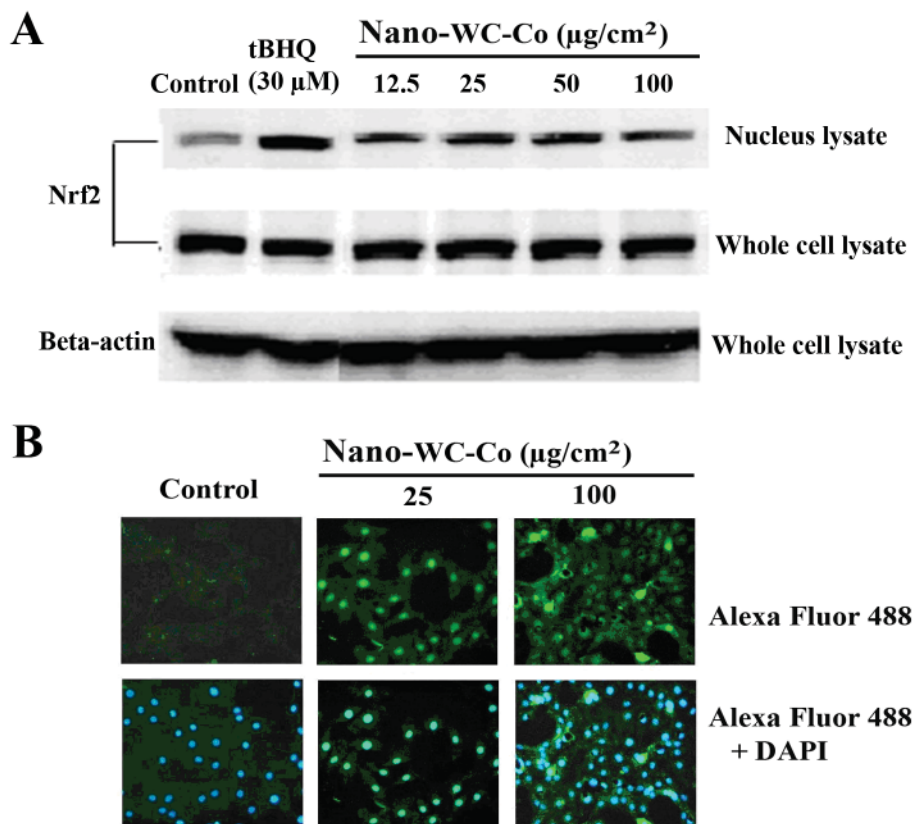


FIGURE 1. Nano-WC-Co particles induced Nrf2 nuclear translocation. JB6 cells were exposed to different doses of nano-WC-Co particles for 5 h. The changes of localization and translocation of Nrf2 were detected by **(A)** western blot and **(B)** immunocytochemistry staining. In **(A)**, tBHQ was used as a positive control, which is frequently used in the induction of Nrf2 nuclear translocation. In **(B)**, green fluorescent dye (Alexa Fluor 488) indicated the Nrf2 localization. The blue fluorescent DAPI was used to stain the nuclei of cells.

significantly enhanced after nano-WC-Co particle treatments (Figs. 3B and 3C).

Effects of ROS on Nano-WC-Co Particle-Induced Nrf2 Target Gene Activation

According to the results obtained above as well as some other early studies,^{20,21} ROS may play an important role in nano-WC-Co particle-induced Nrf2 activation. To verify this hypothesis, ROS generation induced by nano-WC-Co particles was examined by intracellular staining. H₂DCFDA, a general ROS sensitive dye, and DHE, an O₂⁻ specific dye, were used to localize the generation of ROS. Results showed that nano-WC-Co particles induced a strong ROS generation indicated by both H₂DCFDA and DHE staining (Fig. 4). As shown in Fig. 5, catalase, a H₂O₂ scavenging enzyme, exhibited the strongest inhibitory effect on nano-WC-Co particle-induced GST A1 ARE-luciferase activity among the six tested anti-

oxidants, indicating H₂O₂ plays an important role in this process. DFO, a metal ion chelator showed an inhibitory effect, suggesting the involvement of metal ions. NAC, a nonspecific antioxidant that increases glutathione levels, also exhibited inhibitive effects. PVPNO, which can bind to the active surface groups of metal particles, also produced an inhibitory effect. However, SOD, a scavenger of O₂⁻ radical followed by generation of H₂O₂, exhibited no significant inhibition on Nrf2 activity. Sodium formate, an •OH radical scavenger, had no effect on the GST A1 ARE-luciferase activity induced by nano-WC-Co particles. These results indicate that ROS are involved in nano-WC-Co particle-induced Nrf2 activation.

Discussion

Transcription factor Nrf2-mediated antioxidant response represents a critical cellular defense mechanism that serves to maintain intracellular redox ho-

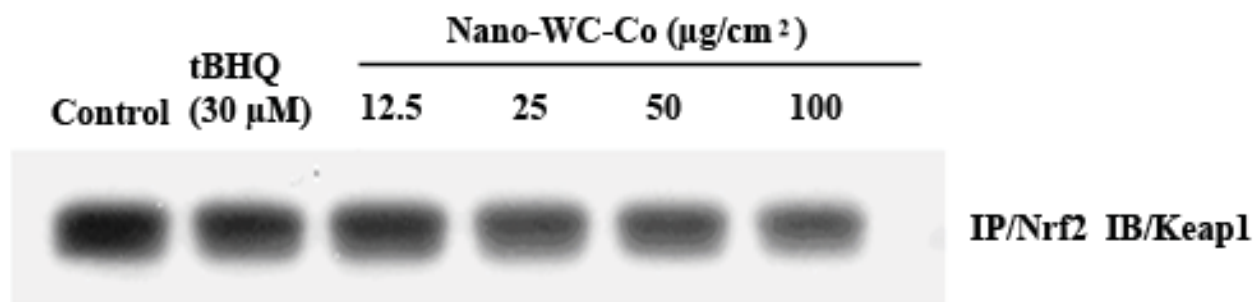


FIGURE 2. Nano-WC-Co particles induced dissociation of Keap1-Nrf2 complexes. JB6 cells were exposed to nano-WC-Co particles for 5 h. IP was then performed using antibody against Nrf2 to obtain Keap1-Nrf2 complex, followed by IB using antibody against Keap1. Keap1 level in nano-WC-Co particle-treated cells was lower than that in the control cells in a dose-dependent manner, which reflects dissociation of Keap1-Nrf2 complexes after stimulation with nano-WC-Co particles.

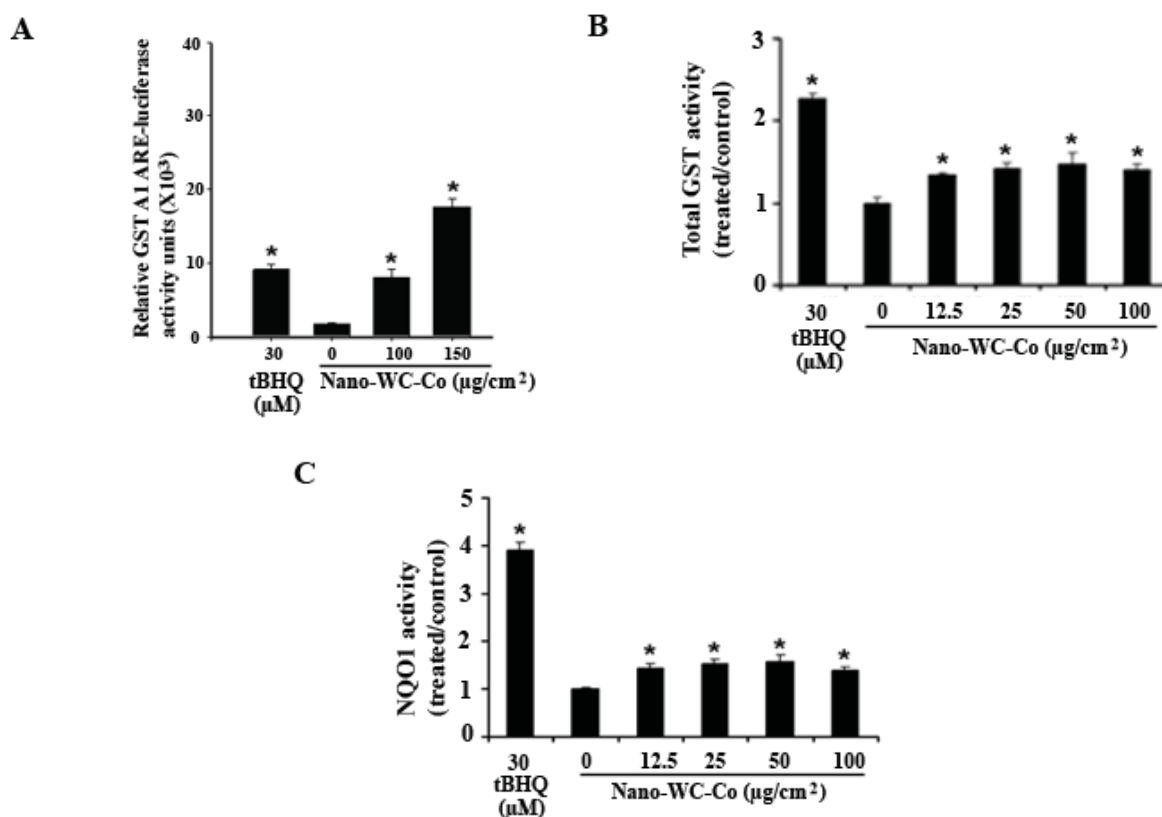


FIGURE 3. Nano-WC-Co particles induced GST and NQO1 gene activation. JB6 cells with luciferase reporter plasmids containing GST A1 ARE were treated with nano-WC-Co particles for 24 h. Thereafter, GST A1 ARE-luciferase activities were measured as described in the Materials and Methods section. Treatment with 30 μM tBHQ was used as a positive control. **(A)** At 100 and 150 $\mu\text{g}/\text{cm}^2$, nano-WC-Co particles induced a significant increase of GST A1 ARE-luciferase activities compared to control. **(B, C)** Measurements of enzymatic activities showed nano-WC-Co particles induced both GST A1 and NQO1 activation. Data shown are means \pm S. E. of three independent assays analyzed by Student's t-test. *Significant increase compared to negative control ($p < 0.05$).

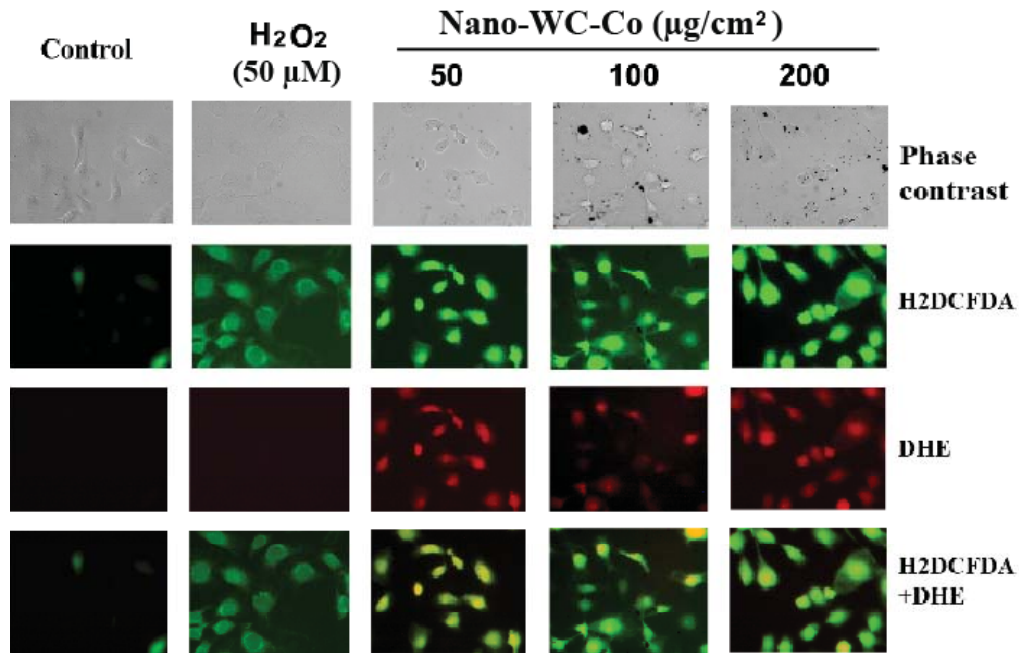


FIGURE 4. Nano-WC-Co particles induced ROS generation. JB6 cells were treated with 50, 100, or 200 $\mu\text{g}/\text{cm}^2$ of nano-WC-Co particles in the presence of 5 μM H2DCFDA and 2 μM DHE for 1 h. The cells were washed three times with PBS followed by addition of fresh medium. The images were captured with a fluorescence microscope. The green color in the cells represents oxidized H2DCFDA, and the red color represents oxidized DHE indicating the intracellular localization of general ROS or $\text{O}_2^{\cdot -}$, respectively. H_2O_2 (50 μM) was used as a positive control.

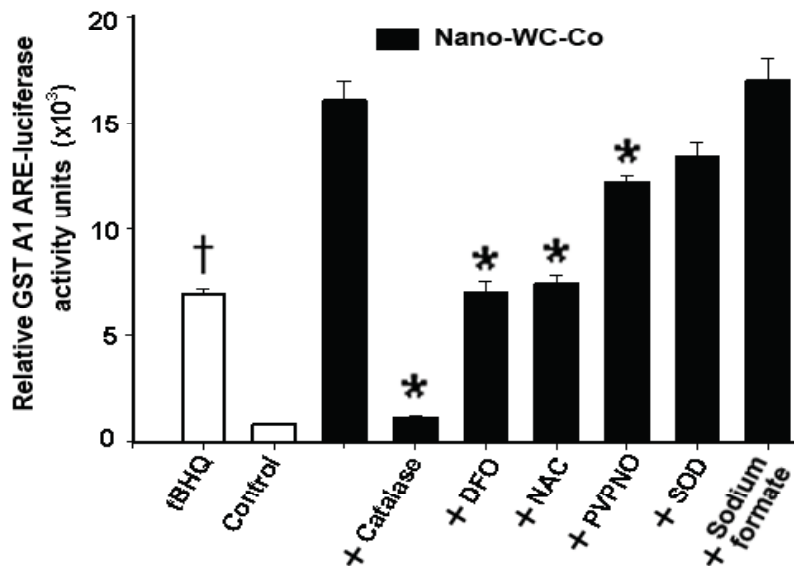


FIGURE 5. Effects of different antioxidants on nano-WC-Co particle-induced Nrf2 target gene activation. To detect the effects of antioxidants on nano-WC-Co particle-induced Nrf2 target gene activation, JB6 cells were pretreated with different antioxidants (catalase 10,000 units/ml, DFO 1 mM, NAC 1 mM, PVPNO 50 $\mu\text{g}/\text{ml}$, SOD 500 units/ml, or sodium formate 2 mM, respectively) for 1 h, and then cells were exposed to nano-WC-Co particles (200 $\mu\text{g}/\text{cm}^2$) for 20 h. The tBHQ (30 μM) was set as a positive control. GST A1 ARE-luciferase activities were measured as described in the Materials and Methods section. Data shown are means \pm S. E. of three independent assays analyzed by Student's t-test. †Significantly higher than negative control ($p < 0.05$). * Significant lower than nano-WC-Co alone ($p < 0.05$).

meostasis and limit oxidative damage.^{12,20,22,23} Recently, Padmanabhan et al.⁹ suggested that Nrf2 may act as a “double-edged sword” in maintenance of redox homeostasis in the human body. Inadequate Nrf2 activity may predispose cells to chemical carcinogenesis because harmful stimulants may not be detoxified. Whereas, aberrant elevated Nrf2 activity may also play a role in the evolution of cancer.^{9,24,25} In the present study, the effects of nano-WC-Co particles on Nrf2 and its downstream gene expressions were investigated in JB6 cells. Exposure of JB6 cells to nano-WC-Co particles resulted in Nrf2 nuclear translocation, as well as a dose-dependent increase in the expression of Nrf2 target genes, including GST and NQO1. Assays using ROS sensitive dyes indicated that ROS were produced in nano-WC-Co particle-treated cells. Pretreatment of the cells with catalase resulted in a strong inhibitory effect on nano-WC-Co particle-induced Nrf2 target gene activation. Our results indicate that activation of Nrf2 signaling pathway in JB6 cells induced by nano-WC-Co particles may be through ROS generation, which implies that ROS may be a major contributor in nano-WC-Co particle-induced adverse health effects.

Nrf2 is normally retained in the cytoplasm via its association with Keap1. Treatment of cells with xenobiotics or antioxidants may lead to the release of Nrf2 from Keap1-Nrf2 complexes.²⁶ Nrf2 translocates into the nucleus and induces the expression of a battery of antioxidant genes.²⁷ Research on non-nanosized metallic Co particles both in human and laboratory studies has shown that exposure to Co can induce excessive production of ROS with subsequent oxidative stress, and that the ROS generation is through a physical-chemical interaction.^{28–31} The cellular response to oxidative stress may be the activation of an Nrf2-mediated series of events, inducing the gene program for the expression of phase II detoxifying enzymes.³² Because cellular reactions to exposures of nano-WC-Co particles could be a serious occupational and public health concern, determining the mechanism of their toxicity is important. In this study, we found that Nrf2 showed a dose-dependent increase in the nuclei of cells treated with nano-WC-Co particles. The disruption of the Keap1-Nrf2 complex and the translocation of Nrf2 were also observed. These results suggest that the signaling pathway of Nrf2/Keap1 is activated following exposure to nano-WC-Co particles. Levels of phase II enzymes (GST A1 and NQO1) were also

enhanced after cells were exposed to nano-WC-Co particles. Further studies indicated that general ROS and $O_2^{\cdot-}$ production were significantly increased in JB6 cells following exposure to nano-WC-Co particles demonstrated by both H2DCFDA and DHE staining.

To detect the involvement of ROS in nano-WC-Co particle-induced Nrf2 target gene activation, effects of different antioxidants on GST A1 ARE-luciferase activity were investigated. The administration of catalase significantly reduced the induction of GST A1 ARE-luciferase activity. DFO, a metal ion chelator, and NAC, a thio-containing antioxidant, also showed some protective effects, but less than catalase. PVPNO, which is used to treat silicosis by its ability to bind to silanol groups on the silica surface, exhibited a slightly protective effect in the present study, and further studies are needed to determine whether it is via the same mechanism as silica. Taken together, inhibitory effects of DFO, NAC, or PVPNO were not as strong as that produced by catalase, suggesting hydrogen peroxide may be the major contributor in ROS induced by nano-WC-Co particles. SOD showed no significant inhibitory effect on nano-WC-Co particle-induced GST activation. The reason may be that though SOD is an $O_2^{\cdot-}$ radical scavenger, it can further promote H_2O_2 generation. Sodium formate did not display any effect, it may be that $\cdot OH$ radical is not involved in nano-WC-Co particle-induced ROS generation.

In summary, exposure of JB6 cells to nano-WC-Co particles activated Nrf2 and its downstream genes, and ROS play an important role in this process. Further studies are necessary to clarify the relationship between Nrf2 activation and carcinogenicity as well as other pathological effects induced by nano-WC-Co particles.

Acknowledgment

This research was supported in part by NIH Grant No. R01ES015518.

Disclaimer

The findings and conclusions in this article have not been formally disseminated by the National Institute for Occupational Safety and Health and should not be considered to represent any agency determination or policy.

References

1. Demedts M, Gyselen A. The cobalt lung in diamond cutters: a new disease. *Verh K Acad Geneeskd Belg.* 1989;51(6):559–81.
2. Lison D. Human toxicity of cobalt-containing dust and experimental studies on the mechanism of interstitial lung disease (hard metal disease). *Crit Rev Toxicol.* 1996 Nov;26(6):585–616.
3. Moulin JJ, Wild P, Romazini S, Lasfargues G, Peltier A, Bozec C, Deguerry P, Pellet F, Perdrix A. Lung cancer risk in hard-metal workers. *Am J Epidemiol.* 1998 Aug 1;148(3):241–8.
4. Nemery B. Metal toxicity and the respiratory tract. *Eur Respir J.* 1990 Feb;3(2):202–19.
5. Kear BH, Skandan G, Sadangi RK. Factors controlling decarburization in HVOF sprayed nano-WC/Co hardcoatings *Scripta Mater.* 2001 May;44(8):1703–7.
6. Venugopal R, Jaiswal AK. Nrf1 and Nrf2 positively and c-Fos and Fra1 negatively regulate the human antioxidant response element-mediated expression of NAD(P)H:quinone oxidoreductase1 gene. *Proc Nat Acad Sci U S A.* 1996 Dec 10;93(25):14960–5.
7. Itoh K, Chiba T, Takahashi S, Ishii T, Igarashi K, Katoh Y, Oyake T, Hayashi N, Satoh K, Hatayama I, Yamamoto M, Nabeshima Y. An Nrf2/small Maf heterodimer mediates the induction of phase II detoxifying enzyme genes through antioxidant response elements. *Biochem Biophys Res Commun.* 1997 Jul 18;236(2):313–22.
8. Hayes JD, McMahon M. The double-edged sword of Nrf2: subversion of redox homeostasis during the evolution of cancer. *Mol Cell.* 2006 Mar 17;21(6):732–4.
9. Padmanabhan B, Tong KI, Ohta T, Nakamura Y, Scharlock M, Ohtsui M, Kang Y, Kobayashi A, Yokoyama S, Yamamoto M. Structural basis for defects of Keap1 activity provoked by its point mutations in lung cancer. *Mol Cell.* 2006 Mar 3;21(5):689–700.
10. Zimniak P, Awasthi S, Awasthi YC. Phase III detoxification system. *Trends Biochem Sci.* 1993 May;18(5):164–6.
11. Kwak MK, Kensler TW, Casero RA Jr. Induction of phase 2 enzymes by serum oxidized polyamines through activation of Nrf2: effect of the polyamine metabolite acrolein. *Biochem Biophys Res Commun.* 2003 Jun 6;305(3):662–70.
12. Kwak MK, Itoh K, Yamamoto M, Sutter TR, Kensler TW. Role of transcription factor Nrf2 in the induction of hepatic phase 2 and antioxidative enzymes in vivo by the cancer chemoprotective agent, 3H-1, 2-dimethiole-3-thione. *Mol Med.* 2001 Feb;7(2):135–45.
13. Lee JM, Li J, Johnson DA, Stein TD, Kraft AD, Calkins MJ, Jakel RJ, Johnson JA. Nrf2, a multi-organ protector? *Faseb J.* 2005 Jul;19(9):1061–6.
14. Zhu H, Jia Z, Zhang L, Yamamoto M, Misra HP, Trush MA, Li Y. Antioxidants and phase 2 enzymes in macrophages: regulation by Nrf2 signaling and protection against oxidative and electrophilic stress. *Exp Biol Med (Maywood).* 2008 Apr;233(4):463–74.
15. Nguyen T, Yang CS, Pickett CB. The pathways and molecular mechanisms regulating Nrf2 activation in response to chemical stress. *Free Radic Biol Med.* 2004 Aug 15;37(4):433–41.
16. Chen XL, Dodd G, Thomas S, Zhang X, Wasserman MA, Rovin BH, Kunsch C. Activation of Nrf2/ARE pathway protects endothelial cells from oxidant injury and inhibits inflammatory gene expression. *Am J Physiol Heart Circ Physiol.* 2006 May;290(5):H1862–70.
17. Itoh K, Ishii T, Wakabayashi N, Yamamoto M. Regulatory mechanisms of cellular response to oxidative stress. *Free Radic Res.* 1999 Oct;31(4):319–24.
18. Chen F, Ding M, Lu Y, Leonard SS, Vallyathan V, Castranova V, Shi X. Participation of MAP kinase p38 and IkappaB kinase in chromium (VI)-induced NF-kappaB and AP-1 activation. *J Environ Pathol Toxicol Oncol.* 2000;19(3):231–8.
19. Feng R, Lu Y, Bowman LL, Qian Y, Castranova V, Ding M. Inhibition of activator protein-1, NF-kappaB, and MAPKs and induction of phase 2 detoxifying enzyme activity by chlorogenic acid. *J Biol Chem.* 2005 Jul 29;280(30):27888–95.
20. Pi J, Zhang Q, Woods CG, Wong V, Collins S, Andersen ME. Activation of Nrf2-mediated oxidative stress response in macrophages by hypochlorous acid. *Toxicol Appl Pharmacol.* 2008 Feb 1;226(3):236–43.
21. He X, Chen MG, Ma Q. Activation of Nrf2 in defense against cadmium-induced oxidative stress. *Chem Res Toxicol.* 2008 Jul;21(7):1375–83.
22. McMahon M, Itoh K, Yamamoto M, Chanas SA, Henderson CJ, McLellan LI, Wolf CR, Cavin C, Hayes JD. The Cap'n'Collar basic leucine zipper transcription factor Nrf2 (NF-E2 p45-related factor 2) controls both constitutive and inducible expression of intestinal detoxification and glutathione biosynthetic enzymes. *Cancer Res.* 2001 Apr 15;61(8):3299–307.
23. Cho HY, Jedlicka AE, Reddy SP, Kensler TW, Yamamoto M, Zhang LY, Kleeberger SR. Role of NRF2 in protection against hyperoxic lung injury in mice. *Am J Respir Cell Mol Biol.* 2002 Feb;26(2):175–82.
24. Shibata T, Kokubu A, Gotoh M, Ojima H, Ohta T, Yamamoto M, Hirohashi S. Genetic alteration of Keap1 confers constitutive Nrf2 activation and resistance to chemotherapy in gallbladder cancer. *Gas-*

- troenterology. 2008 Oct;135(4):1358-68, 68 e1-4.
25. Wang XJ, Sun Z, Villeneuve NF, Zhang S, Zhao F, Li Y, Chen W, Yi X, Zheng W, Wondrak GT, Wang PK, Zhang DD. Nrf2 enhances resistance of cancer cells to chemotherapeutic drugs, the dark side of Nrf2. *Carcinogenesis*. 2008 Jun;29(6):1235-43.
 26. Kensler TW, Wakabayashi N, Biswal S. Cell survival responses to environmental stresses via the Keap1-Nrf2-ARE pathway. *Annu Rev Pharmacol Toxicol*. 2007;47:89-116.
 27. Niture SK, Rao US, Srivenugopal KS. Chemopreventative strategies targeting the MGMT repair protein: augmented expression in human lymphocytes and tumor cells by ethanolic and aqueous extracts of several Indian medicinal plants. *Int J Oncol*. 2006 Nov;29(5):1269-78.
 28. Nemery B, Lewis CP, Demedts M. Cobalt and possible oxidant-mediated toxicity. *Sci Total Environ*. 1994 Jun 30;150(1-3):57-64.
 29. Salnikow K, Su W, Blagosklonny MV, Costa M. Carcinogenic metals induce hypoxia-inducible factor-stimulated transcription by reactive oxygen species-independent mechanism. *Cancer Res*. 2000 Jul 1;60(13):3375-8.
 30. Lison D, Carbonnelle P, Mollo L, Lauwerys R, Fubini B. Physicochemical mechanism of the interaction between cobalt metal and carbide particles to generate toxic activated oxygen species. *Chem Res Toxicol*. 1995 Jun;8(4):600-6.
 31. Lison D, De Boeck M, Verougstraete V, Kirsch-Volders M. Update on the genotoxicity and carcinogenicity of cobalt compounds. *Occup Environ Med*. 2001 Oct;58(10):619-25.
 32. Chen XL, Kunsch C. Induction of cytoprotective genes through Nrf2/antioxidant response element pathway: a new therapeutic approach for the treatment of inflammatory diseases. *Curr Pharm Des*. 2004;10(8):879-91.